

Changes in the trajectory of the radio jet in 0735+178?

J. L. Gómez¹, J. C. Guirado², I. Agudo¹, A. P. Marscher³, A. Alberdi¹,
J. M. Marcaide² and D. C. Gabuzda^{4,5}

¹*Instituto de Astrofísica de Andalucía, CSIC, Apartado 3004, 18080 Granada, Spain*

²*Departamento de Astronomía y Astrofísica, Universidad de Valencia, 46100 Burjassot (Valencia), Spain*

³*Institute for Astrophysical Research, Boston University, 725 Commonwealth Avenue, Boston, MA 02215, USA*

⁴*Joint Institute for VLBI in Europe, Postbus 2, 7990 AA Dwingeloo, The Netherlands*

⁵*Astro Space Center, P. N. Lebedev Physical Institute, Leninsky Prospekt 53, 117924, Moscow, Russia*

ABSTRACT

We present multi-epoch 8.4 and 43 GHz Very Long Baseline Array images of the BL Lac object 0735+178. The images confirm the presence of a twisted jet with two sharp apparent bends of 90° within two milliarcseconds of the core, resembling a helix in projection. The observed twisted geometry could be the result of precession of the jet inlet, but is more likely produced by pressure gradients in the external medium through which the jet propagates. Quasi-stationary components are observed at the locations of the 90° bends, possibly produced by differential Doppler boosting.

Identification of components across epochs, since the earliest VLBI observations of this source in 1979.2, proves difficult due to the sometimes large time gaps between observations. One possible identification suggests the existence of superluminal components following non-ballistic trajectories with velocities up to $11.6 \pm 0.6 h_{65}^{-1} c$. However, in images obtained after mid-1995, components show a remarkable tendency to cluster near several jet positions, suggesting a different scenario in which components have remained nearly stationary in time at least since mid-1995. Comparison with the earlier published data, covering more than 19 years of observations, suggests a striking qualitative change in the jet trajectory sometime between mid-1992 and mid-1995,

with the twisted jet structure with stationary components becoming apparent only at the later epochs. This would require a re-evaluation of the physical parameters estimated for 0735+178, such as the observing viewing angle, the plasma bulk Lorentz factor, and those deduced from these.

Key words:

Techniques: interferometric – galaxies: active – BL Lacertae objects: individual: 0735+178 – Galaxies: jets – Radio continuum: galaxies

1 INTRODUCTION

Radio maps of the BL Lac object 0735+178 ($z = 0.424$, Carswell et al. (1974)) at milliarcsecond resolution obtained using Very Long Baseline Interferometry (VLBI) arrays at centimeter wavelengths show a compact core and a jet of emission extending to the north-east. The first polarimetric VLBI observations of this source were obtained by Gabuzda, Wardle & Roberts (1989) at a wavelength of 6 cm, and revealed a magnetic field predominantly perpendicular to the jet axis. Multi-epoch VLBI observations of 0735+178 (Cotton et al. 1980; Bååth & Zhang 1991; Bååth et al. 1991; Zhang & Bååth 1991; Gabuzda et al. 1994; Gómez et al. 1999) have indicated the existence of superluminal motions with apparent velocities in the range $\simeq 6.5\text{--}12.2 h_{65}^{-1}c$ ($H_0 = 65h_{65} \text{ km s}^{-1} \text{ Mpc}^{-1}$, $q_0 = 0.5$). Gabuzda et al. (1994) observed the intersection of a moving and stationary component, during which there was no evidence for a violent interaction between these features.

The first direct evidence of curved structure in the inner jet of 0735+178 was presented by Kellermann et al. (1998), based on data obtained as part of a Very Long Baseline Array (VLBA) survey at 15 GHz. Polarimetric VLBA observations at 22 and 43 GHz by Gómez et al. (1999) revealed a twisted jet with two sharp apparent bends of 90° within two milliarcseconds of the core. The magnetic field appeared to follow smoothly one of the bends in the jet, interpreted as perhaps produced by a precessing jet nozzle.

In this paper we present new 8.4 and 43 GHz VLBA observations covering three epochs, aimed at studying structural changes in the jet. The higher resolution provided by the 43 GHz observations allows mapping of the inner jet components with an angular resolution of 0.15 mas, through which we can study possible changes in the direction of the jet nozzle in 0735+178. The higher sensitivity at 8.4 GHz provides information about the jet motions in the outer regions, used to test whether components follow ballistic trajectories downstream.

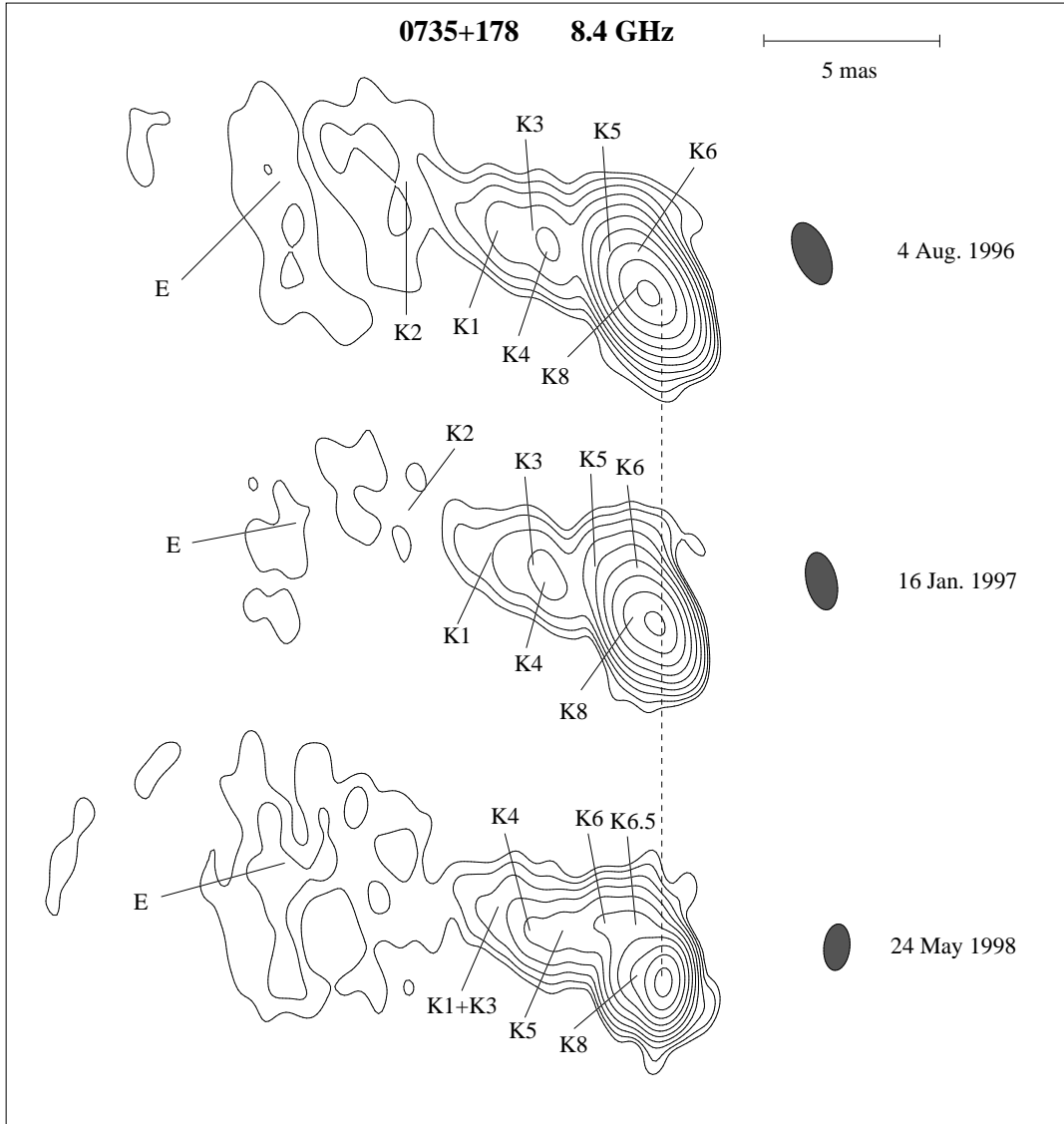


Figure 1. 8.4 GHz VLBA images of 0735+178 at epochs (from *top to bottom*) 4 August 1996, 16 January 1997, and 24 May 1998. Total intensity is plotted as contours. From top to bottom images: contour levels increment by factors of 2, starting at 0.2% (plus 90%), 0.4% (plus 90%), and 0.15% of the peak intensity of 1.05, 1.73, and 2.1 Jy/beam; convolving beams (shown as filled ellipses) are 1.92×0.99 , 1.71×0.88 , and 1.36×0.76 mas, with position angles of 23.6° , 13° , and -6° .

2 OBSERVATIONS

The observations were performed on 4 August 1996, 16 January 1997, and 24 May 1998 using the VLBA at 8.4 and 43 GHz. Left circular polarization data were recorded at each telescope using 8 channels of 8 MHz bandwidth and 1 bit sampling. The reduction of the data was performed within the NRAO Astronomical Image Processing System (AIPS) software in the usual manner (e.g., Leppänen et al. 1995). Opacity corrections for the 43 GHz observations were introduced by solving for receiver temperature and zenith opacity at each antenna.

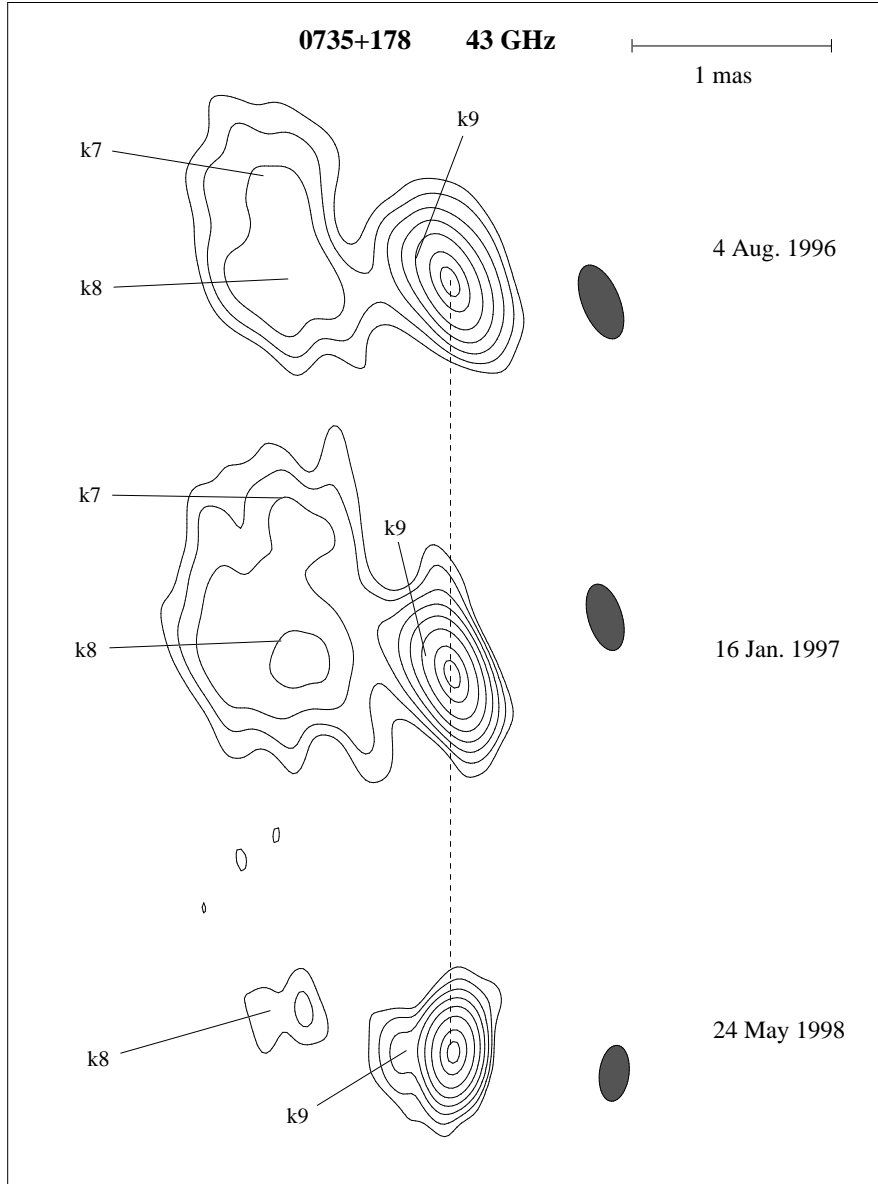


Figure 2. 43 GHz VLBA images of 0735+178 at epochs (from *top to bottom*) 4 August 1996, 16 January 1997, and 24 May 1998. Total intensity is plotted as contours. From top to bottom images: contour levels increment by factors of 2, starting at 2% (including 90%), 1% (plus 90%), and 1% (plus 90%) of the peak intensity of 0.244, 0.361, and 0.791 Jy/beam; convolving beams (shown as filled ellipses) are 0.38×0.18 , 0.33×0.16 , and 0.27×0.14 mas, with position angles of 22.3° , 17° , and -7° .

3 RESULTS

Figures 1 and 2 show the VLBA total intensity images of 0735+178 at 8.4 and 43 GHz, respectively. In order to obtain a better characterization of the motions in the jet, the uv-data were fitted with circular Gaussian components using the Difmap software package (Shepherd 1997). Tables 1 and 2 summarize the physical parameters obtained for 0735+178 at 8.4 and 43 GHz, respectively. The process of model fitting is not deterministic, and often more than one model that fit the data roughly equally well can be obtained for a given data set. Knowledge of the source structure at different observing frequencies and different epochs

Table 1. 8.4 GHz Models for 0735+178.

Component ¹	S (mJy)	r (mas)	θ ($^{\circ}$)	$FWHM$ (mas)
1996.59.				
Core	403 \pm 2	0.0	0.0	\lesssim 0.09
K8	534 \pm 4	0.804 \pm 0.008	76.8 \pm 1.5	0.45 \pm 0.02
K6	78 \pm 4	1.58 \pm 0.03	26.3 \pm 1.3	0.58 \pm 0.12
K5	43 \pm 5	2.15 \pm 0.08	50 \pm 3	0.87 \pm 0.24
K4	15 \pm 3	3.40 \pm 0.21	67 \pm 3	0.9 \pm 0.4
K3	23 \pm 3	4.27 \pm 0.13	65 \pm 2	0.8 \pm 0.3
K1	12 \pm 3	5.48 \pm 0.15	67 \pm 3	0.6 \pm 0.4
K2	\lesssim 8	7.5 \pm 0.9	67 \pm 7	\lesssim 3.7
E	50 \pm 30	10.9 \pm 2.4	72 \pm 8	6.6 \pm 2.3
1997.04.				
Core	542 \pm 11	0.0	0.0	\lesssim 0.3
K8	533 \pm 15	0.836 \pm 0.021	72 \pm 3	0.60 \pm 0.04
K6	65 \pm 11	1.87 \pm 0.23	22 \pm 5	0.71 \pm 0.24
K5	57 \pm 15	2.53 \pm 0.24	52 \pm 6	1.1 \pm 0.5
K4	19 \pm 11	3.7 \pm 0.3	69 \pm 8	\lesssim 2
K3	20 \pm 7	4.21 \pm 0.23	64 \pm 6	\lesssim 1.6
K1	15 \pm 11	5.4 \pm 0.4	67 \pm 8	\lesssim 1.7
K2 ²	\sim 10	\sim 8	\sim 66	\sim 2.4
E	\lesssim 100	11 \pm 3	74 \pm 15	6 \pm 4
1998.39.				
Core	773 \pm 8	0.0	0.0	0.17 \pm 0.04
K8	221 \pm 8	0.835 \pm 0.020	75 \pm 3	0.68 \pm 0.03
K6.5 (K6)	60 \pm 11	1.79 \pm 0.15	23 \pm 3	0.76 \pm 0.13
K6 (K5)	71 \pm 7	2.43 \pm 0.08	46 \pm 3	0.91 \pm 0.16
K5 (K4)	45 \pm 7	3.35 \pm 0.08	64.8 \pm 1.5	0.9 \pm 0.3
K4 (K3)	16 \pm 6	4.24 \pm 0.3	68 \pm 4	\lesssim 1.1
K1+K3 ³ (K1)	\lesssim 30	5.2 \pm 0.3	65 \pm 3	1.2 \pm 0.9
E	\lesssim 150	11.4 \pm 1.5	73 \pm 6	6.6 \pm 2.0

¹Component designations in parantheses correspond to the scenario in which all components are essentially stationary.²Very extended component for which only estimations of the fitted parameters could be obtained.³ In the moving-component scenario, K1 and K3 are merged in a single component with flux density approximately that of the sum of both components for epoch 1997.04.

can help to distinguish among different possible model fits. We have adopted these criteria, selecting the model fits that not only fit best to the source structure for a given epoch and frequency, but are also in best agreement with the known source evolution and structure at different frequencies.

In light of the new observations presented here, we have performed new model fits of the data presented by Gómez et al. (1999). The new model fits are tabulated in Table 3 for the 22 GHz data obtained in 1996.86 and 1996.98, and Table 2 for the corresponding 43 GHz data. These revised model fits result in a better identification of components across epochs, and we have therefore adopted them as the most plausible models for 0735+178. Note, however, that none of the conclusions presented by Gómez et al. (1999) are affected by our adoption of the new model components. The table columns give the total flux density, separation and

Table 2. 43 GHz Models for 0735+178. New model fittings for previous epochs 1996.86 and 1996.98 are also included.

Comp.	S (mJy)	r (mas)	θ ($^{\circ}$)	$FWHM$ (mas)
1996.59.				
Core .	490 \pm 40	0.0	0.0	0.08 \pm 0.04
k9....	100 \pm 40	0.19 \pm 0.04	60 \pm 10	0.16 \pm 0.07
k8....	270 \pm 60	0.78 \pm 0.05	89 \pm 3	0.41 \pm 0.09
k7....	140 \pm 80	1.05 \pm 0.17	60 \pm 7	0.4 \pm 0.3
1996.86.				
Core .	249 \pm 4	0.0	0.0	\lesssim 0.05
k9....	94 \pm 6	0.11 \pm 0.02	81 \pm 15	0.11 \pm 0.04
k8....	229 \pm 6	0.85 \pm 0.02	82 \pm 1	0.49 \pm 0.03
k7....	45 \pm 6	1.22 \pm 0.09	54 \pm 4	0.30 \pm 0.18
k6....	48 \pm 17	1.65 \pm 0.18	24 \pm 7	0.94 \pm 0.33
1996.98.				
Core .	370 \pm 5	0.0	0.0	0.11 \pm 0.03
k8....	222 \pm 8	0.80 \pm 0.04	78 \pm 2	0.70 \pm 0.06
k6 ¹ ...	42 \pm 10	1.49 \pm 0.13	34 \pm 3	0.4 \pm 0.3
k3....	14 \pm 13	3.9 \pm 0.3	62 \pm 9	\lesssim 0.8
1997.04.				
Core .	327 \pm 12	0.0	0.0	\lesssim 0.05
k9....	96 \pm 19	0.158 \pm 0.019	59 \pm 4	0.13 \pm 0.04
k8....	260 \pm 50	0.87 \pm 0.06	80 \pm 4	0.65 \pm 0.06
k7....	47 \pm 22	1.19 \pm 0.13	45 \pm 6	0.4 \pm 0.4
1998.39.				
Core .	536 \pm 8	0.0	0.0	0.059 \pm 0.015
k9....	73 \pm 19	0.189 \pm 0.010	80 \pm 20	0.26 \pm 0.14
k8....	60 \pm 40	0.89 \pm 0.13	78 \pm 10	0.5 \pm 0.3

¹Uncertain identification of this component with K6 at the same epoch.

structural position angle relative to the core component, as well as the FWHM angular size of each component for the three epochs. Components are labeled using uppercase letters for 8.4 GHz following the notation of Gabuzda et al. (1994), and are marked in Figs. 1 and 2. Estimates of the model fitting errors were obtained by using the addendum program for DIFMAP called DIFWRAP, developed by Jim Lovell. The errors were determined by introducing small changes in the fitted parameters of Tables 1, 3, and 2 and analyzing the variations in the residual maps and χ^2 of the fit (see <http://www.vsop.isas.ac.jp/survey/difwrap/> for more details). In order to take into account the fact that the fitted parameters are interrelated, we allowed for simultaneous variations of all four parameters for each component when determining the final errors, which results in somewhat larger but more conservative and perhaps more realistic values.

Table 3. 22 GHz Models for 0735+178 for previous observations in 1996.86 and 1996.98 (Gómez et al. 1999).

Comp.	S (mJy)	r (mas)	θ ($^{\circ}$)	$FWHM$ (mas)
1996.86.				
Core .	292 \pm 8	0.0	0.0	\lesssim 0.01
K9 ...	75 \pm 6	0.18 \pm 0.02	95 \pm 13	0.20 \pm 0.06
K8 ...	192 \pm 6	0.86 \pm 0.02	85 \pm 1	0.51 \pm 0.03
K7 ...	189 \pm 10	0.93 \pm 0.03	61 \pm 3	0.76 \pm 0.05
K6 ...	30 \pm 4	1.66 \pm 0.14	17 \pm 5	0.51 \pm 0.22
K5 ...	25 \pm 6	2.66 \pm 0.17	42 \pm 5	0.99 \pm 0.23
K3 ...	29 \pm 8	4.16 \pm 0.5	65 \pm 6	1.4 \pm 0.5
1996.98.				
Core .	290 \pm 6	0.0	0.0	\lesssim 0.01
K9 ...	55 \pm 3	0.19 \pm 0.03	74 \pm 11	\lesssim 0.01
K8 ...	201 \pm 2	0.89 \pm 0.02	83 \pm 2	0.58 \pm 0.04
K7 ...	132 \pm 2	0.91 \pm 0.03	54 \pm 2	0.84 \pm 0.07
K6 ...	40 \pm 3	1.60 \pm 0.11	20 \pm 5	0.83 \pm 0.21
K5 ...	20 \pm 6	2.47 \pm 0.35	46 \pm 11	0.97 \pm 0.75
K3 ...	23 \pm 6	4.09 \pm 0.25	64 \pm 4	1.04 \pm 0.81

3.1 Changes in the jet trajectory

The images of Figs. 1 and 2 confirm the twisted jet structure previously observed in 0735+178 (Gómez et al. 1999). A first apparent bend of approximately 90° can be observed approximately 0.8 mas from the core, near the position of component K8 (k8 at 43 GHz), where the jet direction changes from eastward to northward, toward component k7. This curvature is more visible in the higher resolution 43 GHz images of Fig. 2. After this, the jet turns back toward the east, as traced by several components identified at 8.4 GHz (see Fig. 1).

Figure 3 summarizes the components detected in 0735+178 since the first observations in 1979. We have split the figure to cover two different time spans. The top plot includes components observed between 1979.20 and 1992.44, while the bottom plot shows component positions after 1995.58 (no observations have been published for epochs between 1992.44 and 1995.58). A zoom showing more clearly the innermost components detected after 1995.58 is plotted in Fig. 4. Independent of the component identification scheme, Fig. 3 shows a qualitative change in the projected trajectory of the jet in 0735+178. In the earlier epochs (top panel of Fig. 3) the jet components appeared to extend along a somewhat rectilinear trajectory to the northeast, while after mid-1995 all observed components lie in a well defined twisted structure, consistent with that mapped in our Figs. 1 and 2, resembling a helix in projection.

3.2 Component identification

We checked to see if any features previously identified in the VLBI jet of 0735+178 were still present in our new images by extrapolating the proper motions detected for components K2 to K6 from previous epochs (Bååth & Zhang 1991; Zhang & Bååth 1991; Bååth, Zhang, & Chu 1991; Gabuzda et al. 1994; Gómez et al. 1999) to our new epochs. This procedure is the basis for the possible component identifications shown in Figs. 1 and 2 (see also Tables 1, 2 and 3). If this identification is correct, K2, K3, K4, K5, and K6 traveled downstream with apparent velocities between $\sim 5\text{--}11\ h_{65}^{-1}$ c. Components K1, K8, and K9 remained stationary within our position error estimates.

At the same time, Figs. 3 and 4 clearly show clustering of components at several locations, labelled in Fig. 4. Thus, the data after the middle of 1995 are also consistent with the VLBI jet of 0735+178 displaying primarily features that are stationary within the estimated position errors. In this case, components K4, K5, K6 and K6.5 of epoch 24 May 1998 would correspond to components K3, K4, K5 and K6 of the two previous epochs, as indicated in Table 1 and Fig. 4. This stationarity of components would contrast with the previously derived superluminal motions, suggesting a possible change in the physical regime for the VLBI jet flow.

It seems very likely that the presence of stationary components at the locations of the two 90° bends (near K8 and K6 Fig. 4) is directly related to the bends in some way. One possibility is that there is differential Doppler boosting in these locations, if these bends are associated with jet regions where the flow velocity vectors are more closely aligned with the line of sight to the observer (e.g. Gómez et al. 1994; Alberdi et al. 2000). Such bends in a highly relativistic flow would be expected to lead to the formation of shocks, which could contribute to enhance the emission at these locations. It is also possible that these bends correspond to jet/external medium interactions, in which case strong shocks are also expected. The stationarity of the remaining components might best be interpreted in terms of standing shock waves. Numerical simulations show that stationary recollimation shocks can be produced by pressure mismatches between the jet and the external medium (Gómez et al. 1995, 1997), as well as by jet instabilities produced by the pass of strong plane perpendicular moving shocks (Agudo et al. 2001). These recollimation shocks result in enhanced jet emission, which could be observed as stationary jet features.

Our new data thus open the possibility that there were mainly stationary features in

the VLBI jet of 0735+178 beginning sometime after the middle of 1992. This may suggest a change in the jet flow regime sometime after mid-1992, since the clustering of components that is clearly visible in the bottom panel of Fig. 3 and in Fig. 4 for epochs after mid-1995 is not evident at earlier epochs. Comparing the models for the most recent VLBI data, the simplest interpretation of the VLBI structure is probably that the jet is made up of a series of stationary or quasi-stationary components. At the same time, a plausible component identification scheme in which the superluminal motions occurring at earlier epochs are continued at the later epochs can be constructed, as discussed above. Clearly, further data are needed to distinguish between these two possibilities.

3.3 Stationary components

Independent of the component identification scheme that is adopted, several components—K1, K8/k8 and k9—have remained stationary within the errors. K1 was initially detected by Bååth & Zhang (1991) at four epochs (their component B). Their first identification for this component lay significantly north of subsequent detections of K1 (see Fig. 3), which would have required a very large apparent motion perpendicular to the observed jet. We therefore suggest that the first identification for component K1 of Bååth & Zhang (1991) may have corresponded to a different jet feature, and we have not included it in our plot for K1 in Fig. 5.

Despite the stationarity of K1, in 1982.83 this component presented a small downstream shift in position, remaining at the new location afterwards, within the errors. The early flux density evolution for K1 (Gabuzda et al. 1994) shows a rapid decrease from 1979.20 to 1980.8, followed by a slower decay until it reaches a 5-GHz flux density of 80 mJy in 1983.5, which is roughly maintained thereafter. Observations at 8.4 GHz since 1990.3 show small variations in the flux density, which always remains below 40 mJy.

Component K8/k8 was first detected in the 1995.58 22-GHz observations of Gabuzda & Cawthorne (2000, their component K1). The sequence of 15 and 22-GHz images from 1996 presented by Homan et al. (2001) shows a component located at a mean distance of 0.8 mas in structural position angle $79.6 \pm 0.7^\circ$, which could also be identified with K8/k8. Although these authors measured a proper motion for this component of 0.14 ± 0.03 mas/yr during 1996, a deceleration is observed in the last epochs. Subsequent observations at 8.4, 22 and 43 GHz confirm the presence of this nearly stationary component (see Figs. 4 and 5).

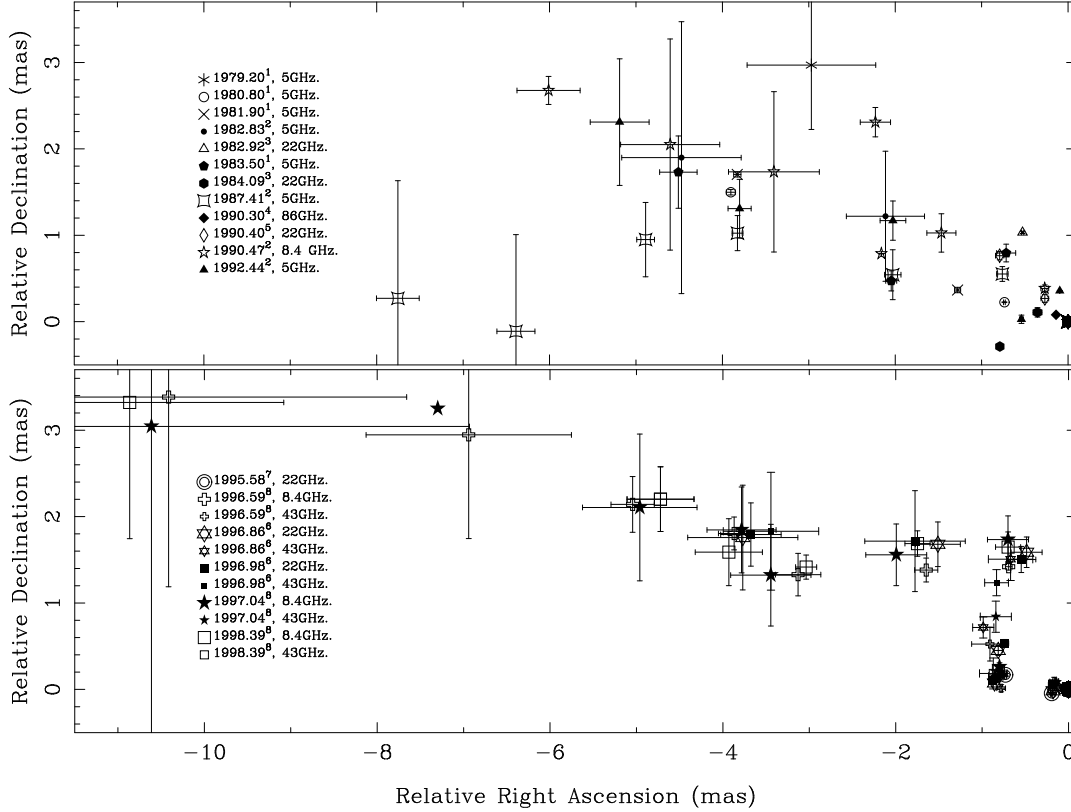


Figure 3. Components position, relative to the core, in the jet of 0735+178 detected between 1979.20 and 1992.44 (*top*), and between 1995.58 and 1998.39 (*bottom*). Epoch, frequency, reference, and symbol for each epoch are as labeled. Estimated errors are indicated by bars. References correspond to: 1. Bååth & Zhang 1991; 2. Gabuzda et al. 1994; 3. Zhang & Bååth 1991; 4. Rantakyrö et al. 1998; 5. Bååth, Zhang, & Chu 1991; 6. Gómez et al. 1999; 7. Gabuzda & Cawthorne 2000; 8. This paper.

K8 has an optically thin spectrum between 8.4 and 43 GHz (see Tables 1 and 2), although observations at 22 and 43 GHz show a slightly inverted spectrum between these frequencies, which we find puzzling. Figure 2 reveals that k8 is extended (see also Tables 1, 2, and 3). It therefore seems likely that the “wandering” of its position should be interpreted not as physical motion, but rather as the result of internal changes in the component’s brightness distribution, which lead to small shifts in the position of the brightness centroid as a function of frequency and epoch.

The innermost stationary component in 0735+178, k9, is ~ 0.2 mas from the core. Only observations above 22 GHz provide the necessary resolution to detect it. It has an inverted spectrum and, like K8, shows small variable offsets in position with epoch and frequency, which we also interpret as the effect of changes in its internal brightness distribution. Observations at 86 GHz by Rantakyrö et al. (1998) in 1990.3 revealed two strong components separated by 0.16 mas. Although those observations and the observations of Gabuzda & Cawthorne (2000) are more than five years apart, it is possible that component A of Rantakyrö et al. (1998) should be identified with component K2 of Gabuzda & Cawthorne

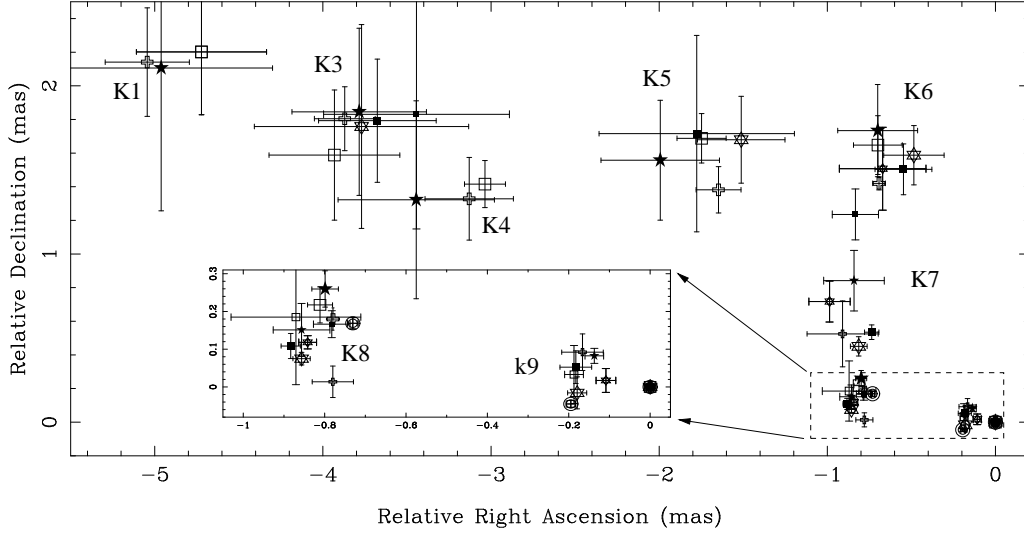


Figure 4. Zoom of the inner components detected between 1995.58 and 1998.39 (bottom panel in Fig. 3). Symbols are as in Fig. 3, and labels correspond to the stationary-component scenario.

(2000) and our component k9, suggesting that it has remained stationary for at least eight years. This component has a quasi-steady flux density and inverted spectrum.

Images at 22 and 43 GHz show a “bridge” of emission extending north to connect component K8/k8 with the second 90° bend located near the position of component K6 at epoch 1996.59. We have model fitted this emission and identified it across epochs as k7. If component motions in 0735+178 are non-ballistic, various components should have moved through the two apparent 90° bends at the positions of K8/k8 and K6, through where the emission modelled as k7 is observed. However, k7 exhibits erratic motions around the extended region, as indicated by the errors in its position. This may suggest that what we have modelled as k7 actually corresponds to underlying jet emission rather than a distinct feature in the flow. This region has a steep spectrum between 22 and 43 GHz.

The 8.4 GHz images in Fig. 1 show extended jet emission (with flux density below ~ 150 mJy) to the east of K2. To account for this flux density, we have fitted its emission as a single component, labeled E, which has a rather large flux density. Due to its very extended structure, the errors in the model fitting are quite large. We emphasize that this is only intended to allow for the presence of the extended emission in this region in a general sense.

3.4 Possible Superluminal components

As discussed above, probably the simplest interpretation of the VLBI structure observed at relatively recent epochs is that it is made up of a series of stationary or quasi-stationary

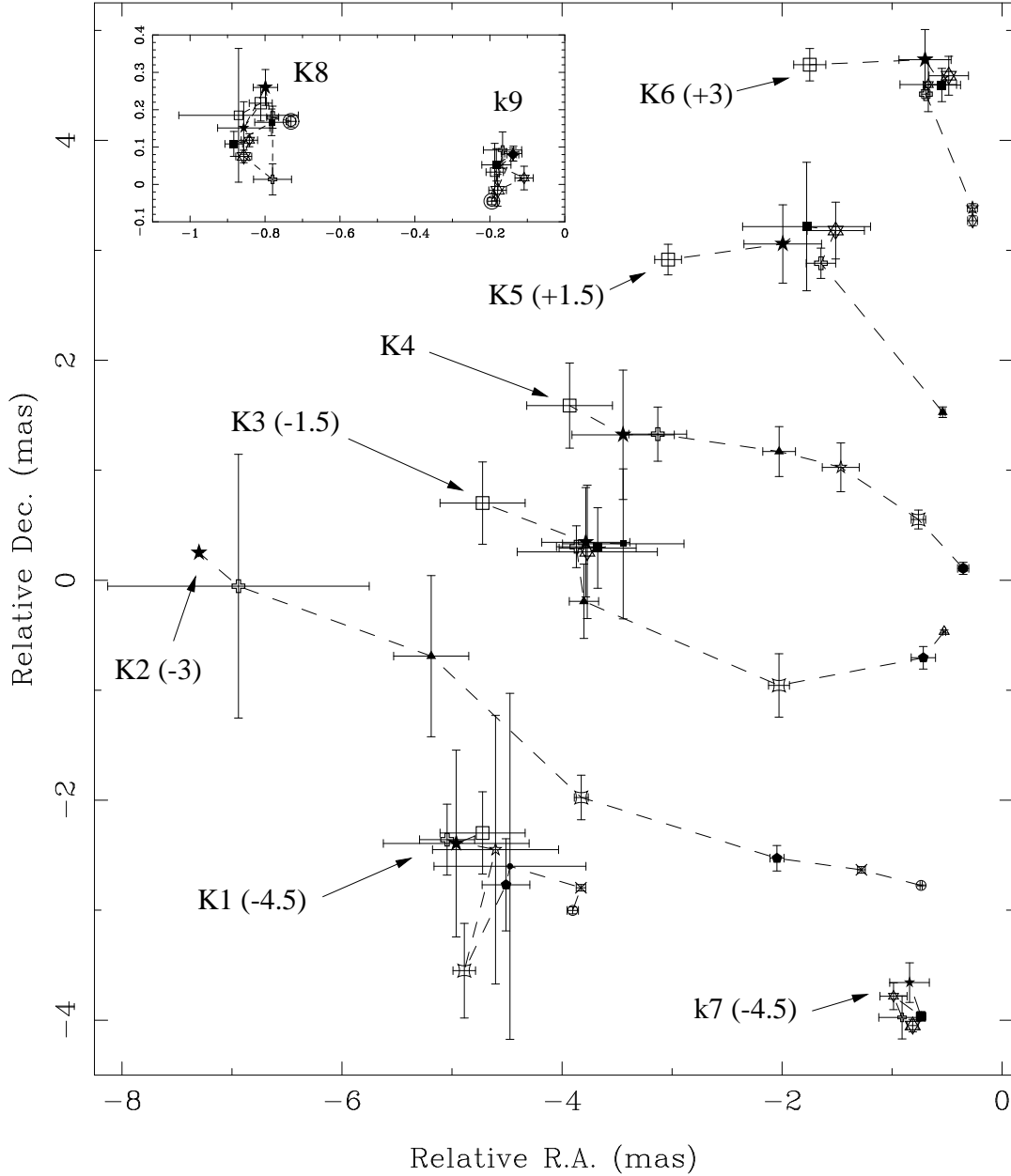


Figure 5. Apparent trajectories of components in 0735+178. Symbols used are the same of Fig. 3. For clarity, components positions have been shifted in declination by the amount (in milliarcseconds) expressed in parentheses. Inset panels shows the fitted positions for components K8 (k8 at 43 GHz) and k9. Dashed lines connect the positions of the different components across epochs.

components. At the same time, we can plausibly identify components across epochs in a way that implies superluminal motions similar to those estimated for earlier epochs. In this case (corresponding to the component labels in Fig. 1), components K2, K3, K4, K5 and K6 all exhibit superluminal motion. As shown in Fig. 5, all of these components seem to follow curved paths, especially K5 and K6.

When estimating a component's implied trajectory, we averaged the positions obtained at different frequencies and nearby epochs. In this way, we derived mean positions for com-

ponents detected at 1990.40 and 1990.47, and for 1996.86, 1996.98, and 1997.04. Typically, components expand as they move from the core, resulting in larger errors in the model fitting. To account for such variations in the position errors, we obtained a weighted mean value for the apparent motions using the inverse square errors as weights. When computing the apparent speed, we allowed for motion along non-rectilinear paths, and calculated the distance traveled in the plane of the sky.

In this “moving-component” scenario, the first detection of K2 corresponds to observations at 5 GHz by Bååth & Zhang (1991, their component C0). Observations at 5 GHz by Gabuzda et al. (1994) in 1992.44 showed a component at a distance of 5.68 mas from the core that they tentatively identified with component K1. However, comparison with later epochs suggests that this component may fit the trajectory and flux density evolution of K2 better, and therefore we consider this identification more plausible. Overall, the trajectory for K2 is consistent with quasi-ballistic motion along position angle 70° . At epoch 1997.04, we could only obtain estimates of the flux density and position of extended jet emission at the position expected for K2. Due to the large errors associated with this component at this epoch, no errors bars have been plotted in Figs. 3 and 5. The light curve for component K2 shows a smooth decay with time. The analysis described above yields an apparent speed for K2 of $11.6 \pm 0.6 h_{65}^{-1} c$.

Overall, K3 follows a similar path to that of K2, but with a slower mean apparent velocity of $8 \pm 1.5 h_{65}^{-1} c$. Our last epoch suggests that K3 reached the position of K1, as reported previously for K2 by Gabuzda et al. (1994). As in the K2+K1 intersection observed by Gabuzda et al. (1994), our images do not show evidence of a violent interaction between components K3 and K1. Table 1 suggests that the flux density of the merged K3 and K1 is approximately that of the sum of the two separate components at epoch 1997.04. As shown in Fig. 5, K1 remained stationary (within the errors) during its intersection with K3. We note that the inferred motion for K3 fluctuates between 1992.4 and 1998.4; this may providing indirect evidence in favour of our alternative scenario, in which the VLBI structure observed in recent epochs is made up of stationary or quasi-stationary components.

Component K4 was first detected by Zhang & Bååth (1991) in 1984.09 (their component 2), 0.37 mas from the core. As shown in Fig. 5, the inferred trajectory is curved, and is consistent with that outlined by the components in Figs. 3 and 4. However, more frequent monitoring during its initial evolution would have been necessary to test for the presence of non-ballistic motion through the inner bends. The inferred flux density of K4 shows a

monotonic decrease with time, as expected for adiabatic evolution. This component’s mean apparent speed is $5 \pm 1h_{65}^{-1}c$.

Figure 5 shows that the moving-component scenario suggests very non-ballistic trajectories for K5 and K6; however, this is based on an uncertain identification with components at previous epochs. A time gap of about 4.5 years separates the observations of Gabuzda et al. (1994) and of Gómez et al. (1999; also Table 3). Our estimated apparent speeds of 10 ± 3.5 and $4.6 \pm 0.1h_{65}^{-1}c$ for K5 and K6, respectively, are accordingly severely affected by this uncertainty in the identifications with features at the earlier epochs. Component K6 was initially identified as K5 at epoch 1990.47 by Gabuzda et al. (1994) based on its separation from the core. However, if we take into account its structural position angle for that epoch, this component fits better with the overall evolution of K6, and we have therefore identified it accordingly.

When analysing our images together with those published previously, we tried to make our component identifications as consistent as possible with those proposed by other authors. At the same time, due to the large time gaps between some of the observing epochs, as well as the possible change in the jet geometry that seems to have occurred in one of these gaps, there are several components detected in earlier studies that do not fit easily the behaviour inferred for our identified components. Those include component B of Bååth & Zhang (1991); component 3 of Zhang & Bååth (1991); component C2 of Bååth, Zhang, & Chu (1991); and components K2 (1982.83), C2 (1990.47), K3 (1990.47), K2.5 (1990.47), and K6 (1992.44) of Gabuzda et al. (1994). Some of these are from rather early VLBI observations, and it may not be surprising if the corresponding images and model fits were not entirely accurate representations of the true source structure. In our “moving components” scenario, K6.5 is not identified with any components seen in our or other studies, but it is identified with the quasi-stationary component K6 in our “stationary components” scenario.

4 DISCUSSION

Although it is quite common to observe relatively strong curvature in the jets of compact AGN, the very twisted geometry found in 0735+178 presents a somewhat dramatic and peculiar example, due to the presence of two 90° bends in the inner two mas of the VLBI jet. In addition, comparison with previous observations suggests that the jet geometry has changed with time. Figure 3 reveals two distinct jet geometries before and after the middle

of 1992. The observations of Gabuzda & Cawthorne (2000) for 1995.58 and of Homan et al. (2001) for several epochs in 1996 are consistent with the twisted inner jet geometry seen in our later images, although they show only the inner 1 mas of the jet structure. The 5-GHz VLBA observations of Nan Rendong and collaborators at epoch 1995.33 (private communication) also confirm the presence of the two 90° bends, suggesting that if the jet in 0735+178 did experience a change in flow regime, this occurred sometime between mid-1992 and mid-1995.

It seems likely that the apparent bending of the relativistic jet is so abrupt (two bends through roughly 90°) because we are viewing the jet of 0735+178 at a small angle to the line of sight, so that intrinsic curvature is enhanced by projection effects. The intrinsic bending could be produced either by a change in the direction of ejection (e.g., jet precession or by other more erratic variations) or by gradients in the external pressure that are not aligned with the initial direction of the jet flow. Precession of the jet could lead to either ballistic (as observed in SS 433) or non-ballistic fluid motions, in which the flow velocity vector would follow the jet bends. Three-dimensional numerical simulations of precessing jets (Aloy et al. 1999, 2000) can give rise to helical structures, as produced by normal mode jet instabilities, and have been applied to interpret the variability observed in several sources (Hardee 2000). Non-ballistic motions would be expected in this case.

Is the jet of 0735+178 precessing? Jet precession should lead to changes in the inner jet geometry, as well as to components being ejected in different position angles at different times, if the time scale for the precession is comparable to that covered by the observations. Our observations suggest a change in the apparent jet geometry in 0735+178, but the initial quasi-rectilinear geometry observed in relatively early images does not appear to be consistent with a precessing jet scenario. There is no clear and consistent evidence that different components have been ejected in systematically different directions with time, as would be expected for a precessing jet. In addition, we find evidence for a number of stationary components; if our identification of component k9 with component A of Rantakyrö et al. (1998) is correct, this component remained stationary for more than eight years. A jet precessing in such a way as to lead to the observed twisted inner-jet structure would require that k9 experience significant changes in its position angle with respect to the core, as well as flux variability, which are not observed. For this reason, it is most likely that the jet of 0735+178 is not precessing, but additional observations are needed to more conclusively test this hypothesis.

Are components in the jet of 0735+178 ballistic? Although earlier model fits were consistent with roughly ballistic motion for a number of components, our analysis of our more recent data indicates that either (1) the components in the VLBI jet of 0735+178 have been roughly stationary at least since mid-1995 or (2) the VLBI jet components move superluminally along curved paths. The possible co-existence of standing and moving features is more consistent with non-ballistic component motions; the stationary components could be associated with bends in the jet, as in the case of the quasi-stationary components K8 (at the first 90° bend, where the jet turns toward the north) and K6 (at the second 90° bend, where the jet turns back toward the east). In addition, the jet of 0735+178 has stationary components in regions where there is no apparent curvature. The proximity to the core of the stationary component k9 suggests that it may be produced by a recollimation shock rather than a bend. Relativistic numerical simulations (Agudo et al. 2001) suggest that this type of stationary component, produced by jet instabilities, should be common.

Overall, the stability of the jet structure over the many epochs of observations made since mid-1995 (Fig. 4) suggests that these images show a series of quasi-stationary components, making the possibility that we are actually viewing a superposition of linear ballistic trajectories that “conspire” to produce the observed structure unlikely. The polarimetric observations of Gómez et al. (1999) showed a longitudinal magnetic field in the jet, which appeared to follow the curvature observed near K6, also supporting a picture with non-ballistic fluid motions.

Since precession of the jet seems unlikely, it is more plausible that the twisted geometry of 0735+178 is the result of pressure gradients in the external medium through which the jet propagates, possibly triggered by its own interaction with the ambient medium. In this case, we might expect gradual changes in the position and curvature of the jet bends near K8 and K6 with time. Evidence for the existence of such pressure gradients on VLBI scales is provided, for example, by the jet/external medium interactions observed in the radio galaxy 3C 120 (Gómez et al. 2000), the compact steep-spectrum source 3C 119 (Nan et al. 1999), the quasar 1055+018 (Attridge et al. 1999), and the BL Lac object 0820+225 (Gabuzda et al. 2001), and also the detection of non-uniform parsec-scale rotation measures in a growing number of active galactic nuclei (Nan et al. 1999; Taylor 1998, 2000; Zavala & Taylor 2001; Gabuzda et al. 2001; Reynolds et al. 2001).

The most intriguing result revealed by data obtained since mid-1995 is the appearance of distinct clustering of components near several jet locations. Although it is possible to

derive a component identification scheme for these recent images in which components move superluminally, this clustering of components suggests instead a transition to a jet flow regime that has led to the formation of a series of quasi-stationary regions of emission. The clustering is rather stable, and it is unlikely that it could arise by chance, due to particular epochs “catching” components right at certain specific jet locations. This component clustering opens a new view of 0735+178, in which essentially all jet components remain nearly stationary with time, or at least have much smaller proper motions than measured previously. This would require a re-evaluation of the physical parameters estimated for 0735+178 from measuring proper motions, such as the observing viewing angle, plasma bulk Lorentz factor, and those deduced from these.

The reason for the absence of this clustering of jet components in earlier images remains unclear. It probably cannot be excluded that the quality of the earlier images was such that the sharply twisted jet structure with quasi-stationary regions of emission was present but remained undetected. However, the second sharp bend is located well to the north of the core, and it seems unlikely that it would not have been detected in any of the earlier images, especially since some of the pre-1993 images were made at 22 GHz. It seems more likely that the jet of 0735+178 experienced a change in flow regime sometime between mid-1992 and mid-1995. If so, this is the first time that such a transition has been observed. Continued monitoring of the VLBI structure of 0735+178 is clearly of interest, both in order to obtain further information about the origin of the twisted jet structure visible in our images, and to see if the jet may make another transition in flow regime that leads to the break-up of this stable twisted structure.

ACKNOWLEDGMENTS

This research was supported in part by Spain’s Dirección General de Investigación Científica y Técnica (DGICYT) grants PB97-1164 and PB96-0782, by U.S. National Science Foundation grant AST-9802941, and by the Fulbright commission for colabration between Spain and the United States. DCG acknowledges support from the European Commission under the IHP Programme (ARI) contract No. HPRI-CT-1999-00045.

REFERENCES

- Agudo, I., Gómez, J. L., Martí, J. M., Ibáñez, J. M., Marscher, A. P., Alberdi, A., Aloy, J. M. & Hardee P. E. 2001, *ApJ*, 549, L183
- Alberdi, A., Gómez, J. L., Marcaide, J. M., Marscher, A. P., Pérez-Torres, M. A. 2000, *A&A*, 361, 529
- Aloy, M. A., Ibáñez, J. M., Martí, J. M., Gómez, J. L. & Müller, E. 1999, *ApJ*, 523, L125
- Aloy, M. A., Gómez, J. L., Ibáñez, J. M., Martí, J. M. & Müller, E. 2000, *ApJ*, 528, L85
- Attridge, J. M., Roberts, D. H., & Wardle, J. F. C. 1999, *ApJ*, 518, L87
- Bååth, L. B. & Zhang, F. J. 1991, *A&A*, 243, 328
- Bååth, L. B., Zhang, F. J. & Chu, H. S. 1991, *A&A*, 250, 50
- Carswell, R. F., Strittmatter, P. A., Williams, R. D., Kinman, T. D. & Serkowski, K. 1974, *ApJ*, 190, L101
- Cotton, W. D., Wittels, J. J., Shapiro, I. I., Marcaide, J., Owen, F. N., Spangler, S. R., Rius, A., Angulo, C., Clark, T. A. & Knight, C. A. 1980, *ApJ*, 238, L123.
- Gabuzda, D. C. & Cawthorne, T. V. 2000, *MNRAS*, 319, 1056
- Gabuzda, D. C., Pushkarev, A. B., & Garnich, N. N. 2001, *MNRAS*, in press
- Gabuzda, D. C., Wardle, J. F. C. & Roberts, D. H. 1989, *ApJ*, 338, 743
- Gabuzda, D. C., Wardle, J. F. C., Roberts, D. H., Aller, M. F. & Aller, H. D. 1994, *ApJ*, 435, 128
- Gómez, J. L., Alberdi, A., Marcaide, J. M., Marscher, A. P. & Travis, J. P. 1994, *A&A*, 292, 33
- Gómez, J. L., Martí, J. M., Marscher, A. P., Ibáñez, J. M. & Marcaide, J. M. 1995, *ApJ*, 449, L19
- Gómez, J. L., Martí, J. M., Marscher, A. P., Ibáñez, J. M. & Alberdi, A. 1997, *ApJ*, 482, L33
- Gómez, J. L., Marscher, A. P., Alberdi, A., Gabuzda, D. C. 1999, *ApJ*, 519, 642
- Gómez, J. L., Marscher, A. P., Alberdi, A., Jorstad, S. G. & García-Miró, C. 2000, *Science*, 289, 2317
- Hardee, P. E. 2000, *ApJ*, 533, 176
- Homan, D. C., Ojha, R. Wardle, J. F. C., Roberts, D. H., Aller, M. F., Aller, H. D. & Hughes, P. A. 2001, *ApJ*, in press (available as astro-ph/0009301)
- Kellermann, K. I., Vermeulen, R. C., Zensus, J. A. & Cohen, M. H. 1998, *AJ*, 115, 1295
- Leppänen, K. J., Zensus, J. A. & Diamond, P. J. 1995, *AJ*, 110, 2479
- Nan, R. D., Gabuzda, D. C., Kamenov, S., Schilizzi, R. T., & Inoue, M. 1999, *A&A*, 344, 402.
- Reynolds, C., Cawthorne, T. V., & Gabuzda, D. C. 2001, *MNRAS*, in press.
- Rantakyrö, F. T. et al. 1998, *A&AS*, 131, 451
- Shepherd, M. C. 1997, in *Astronomical Data Analysis Software and Systems VI*, Astron. Soc. Pac. Conf. Proc., 125
- Taylor, G. B. 1998, *ApJ*, 506, 637
- Taylor, G. B. 2000, *ApJ*, 533, 95
- Zavala, R. T. & Taylor, G. B. 2001, *ApJ*, 550, L147
- Zhang, F. J. & Bååth, L. B. 1991, *MNRAS*, 248, 566